



Published in final edited form as:

Cancer Res. 2011 July 15; 71(14): 4866–4876. doi:10.1158/0008-5472.CAN-10-4576.

CCI-779 Inhibits Cell-Cycle G2/M Progression and Invasion of Castration Resistant Prostate Cancer via Attenuation of UBE2C Transcription and mRNA Stability

Hongyan Wang¹, Chunpeng Zhang², Anna Rorick², Dayong Wu², Ming Chiu¹, Jennifer Thomas-Ahner³, Zhong Chen², Hongyan Chen², Steven K. Clinton³, Kenneth K. Chan¹, and Qianben Wang²

¹Division of Pharmaceutical Sciences, College of Pharmacy, The Ohio State University, Columbus, Ohio

²Department of Molecular and Cellular Biochemistry, College of Medicine, The Ohio State University, Columbus, Ohio

³Division of Medical Oncology, Department of Internal Medicine, College of Medicine, The Ohio State University, Columbus, Ohio

Abstract

The cell-cycle G2/M phase gene *UBE2C* is over-expressed in various solid tumors including castration-resistant prostate cancer (CRPC). Our recent studies found *UBE2C* to be a CRPC-specific androgen receptor (AR) target gene that is necessary for CRPC growth, providing a potential novel target for therapeutic intervention. Here we demonstrate that the G1/S cell-cycle inhibitor-779 (CCI-779), an mTOR inhibitor, inhibited *UBE2C* mRNA and protein expression in AR-positive CRPC cell models abl and C4-2B. Treatment with CCI-779 significantly decreased abl cell proliferation *in vitro* and *in vivo* through inhibition of cell-cycle progression of both G2/M and G1/S phases. In addition, exposure of abl and C4-2B cells to CCI-779 also decreased *UBE2C*-dependent cell invasion. The molecular mechanisms for CCI-779 inhibition of *UBE2C* gene expression involved a decreased binding of AR co-activators SRC1, SRC3, p300 and MED1 to the *UBE2C* enhancers, leading to a reduction in RNA polymerase II loading to the *UBE2C* promoter, and attenuation of *UBE2C* mRNA stability. Our data suggest that, in addition to its ability to block cell-cycle G1/S transition, CCI-779 causes a cell-cycle G2/M accumulation and an inhibition of cell invasion through a novel *UBE2C*-dependent mechanism, which contributes to anti-tumor activities of CCI-779 in *UBE2C* over-expressed AR-positive CRPC.

Keywords

CCI-779; G2/M arrest; invasion; *UBE2C*; castration-resistant prostate cancer

Introduction

The androgen receptor (AR), a ligand-dependent transcription factor, is expressed in both androgen-dependent prostate cancer (ADPC) and castration-resistant prostate cancer

Corresponding Author: Qianben Wang, Department of Molecular and Cellular Biochemistry and Comprehensive Cancer Center, The Ohio State University, 888 Biomedical Research Tower, 460 W. 12th Avenue, Columbus, OH 43210. Phone: 614-247-1609; Fax: 614-688-4181; qianben.wang@osumc.edu. .

Disclosure of Potential Conflicts of Interest

No potential conflicts of interest were disclosed.

(CRPC) (1, 2). One important function of AR in prostate cancer is to drive cell-cycle progression (3). While it is well known that AR mainly regulates cell-cycle G1/S transition in ADPC through AR-dependent regulation of CCND1, p21 and p27 (3), recent integrated analysis of AR cistrome and gene expression data in prostate cancer found that AR selectively binds to the enhancers of G2/M phase genes in CRPC but not in ADPC, leading to higher G2/M phase gene expression and accelerated cell-cycle G2/M progression in CRPC versus ADPC (4, 5).

One of such AR-regulated G2/M phase genes in CRPC is *UBE2C*, a gene whose translation product is an anaphase promoting complex/cyclosome (APC/C)-specific E2 ubiquitin-conjugating enzyme (6). Significantly, *UBE2C* mRNA and protein expression levels are overexpressed in CRPC cases (4, 7, 8). Consistent with the essential role of *UBE2C* in driving M-phase cell cycle progression by inactivating the M-phase check point (9) or increasing the pool of active APC/C (10), silencing of *UBE2C* in CRPC cells arrests cell-cycle in G2/M phase and decreases CRPC cell proliferation, suggesting that *UBE2C* is a potential therapeutic target for CRPC (4).

Here, we screened several clinically active compounds for their ability to decrease *UBE2C* expression. CCI-779 (cell cycle inhibitor-779; temsirolimus), an ester analog of mTOR inhibitor rapamycin currently under clinical evaluation (11), emerged from screening to have significant efficacy and potency in inhibition of *UBE2C* protein and mRNA expression in AR-positive CRPC cell lines abl and C4-2B. Although previous studies found that mTOR inhibitors including CCI-779 decreases the growth of cancer cell lines (e.g. AR-negative CRPC cell lines PC-3 and DU-145) via G1/S inhibition (12, 13), we show that CCI-779 inhibits the abl *in vitro* and *in vivo* growth by blocking both cell-cycle G2/M and G1/S transitions. Consistent with the newly identified role of *UBE2C* in promoting tumor invasion and metastasis (14-16), we find that CCI-779 treatment decreases *UBE2C*-dependent cell invasion of abl and C4-2B cells. Finally, we find that the combined effects on attenuating *UBE2C* transcription and mRNA stability of CCI-779 lead to decreased mRNA levels of *UBE2C*. Collectively, this study identifies CCI-779 as a *UBE2C* inhibitor in CRPC.

Materials and Methods

Reagents and cell culture

CCI-779 (temsirolimus) was purchased from LC Laboratories (Woburn, MA). LNCaP cells were obtained from American Type Culture Collection (ATCC) and C4-2B cells were purchased from ViroMed Laboratories (Minneapolis, MN). LNCaP and C4-2B cells were cultured in RPMI1640 media (Invitrogen, Carlsbad, CA) supplemented with 10% FBS and authenticated by the suppliers. abl cells, androgen-independent derivative of LNCaP cell line, were kindly provided by Zoran Culig (Innsbruck Medical University, Austria) and authenticated by Culig laboratory using AR sequence analysis, cytogenetic analysis and CGH analysis (17). The abl cells were maintained in RPMI1640 media containing 10% charcoal-stripped FBS. All three cell lines were passaged in our laboratory for less than 6 months after resuscitation.

Western blot

Cells or tumor tissues were collected and lysed as previously described (18). The total lysate sample (50 µg per lane) was resolved by SDS-PAGE and immunoblotted with primary antibodies. Antibodies against various proteins were purchased from the following sources: anti-*UBE2C* (A650) from Boston Biochem (Cambridge, MA); anti-AR (441), anti-GATA2 (H116), anti-SRC1 (M341), anti-p300 (C20), anti-MED1 (M255) from Santa Cruz Biotechnology (Santa Cruz, CA); anti-CCND1 (ab24249) and anti-FoxA1 (ab23738) from

Abcam (Cambridge, MA); anti-calnexin from Stressgen (Victoria BC, Canada), and anti- β -actin from Sigma-Aldrich (St. Louis, MO). An anti-SRC3 antibody has been described previously (19).

Real-time RT-PCR

Total RNA was isolated from cells using Trizol reagent (Invitrogen). Real time RT-PCR was performed on 100 ng of RNA by using MultiScribe reverse transcriptase and SYBR Green PCR kit (Applied Biosystems, Foster City, CA) according to the manufacturer's protocol. The following primers were used: UBE2C (5'-TGGTCTGCCCTGTATGATGT-3' and 5'-AAAAGCTGTGGGGTTTTTCC-3') (20); CCND1 (5'-TCCTCTCCAAAATGCCAGAG-3' and 5'-GGCGGATTGGAAATGAACTT-3'), GAPDH (5'-TCCACCCATGGCAAATTC-3' and 5'-TCGCCCACTTGATTTTGG-3') (19), and actin (5'-AGGCACCAGGGCGTGAT-3' and 5'-GCCACATAGGAATCCTTCTGAC-3')(21).

RNA interference

ON-TARGET plus™ siRNAs targeting CCND1 and UBE2C (siCCND1 and siUBE2C) and ON-TARGET plus™ control siRNA (siControl) were purchased from Dharmacon (Lafayette, CO). siRNAs were transfected using Lipofectamine 2000 (Invitrogen, Carlsbad, CA).

Synchronization and fluorescence-activated cell sorting (FACS) analysis

Cells were arrested in G2/M phase by using a thymidine-nocodazole block as previously described (22). Briefly, cells were first synchronized by arresting them at the G1/S border with 2 mM thymidine for 24 hours, followed by a 4-hour release, and then arrested at M phase with 100 ng/ml nocodazole for 12 hours. CCI-779 (50 nM) or vehicle control was added at the same time as nocodazole. The cells were released from the nocodazole block with two washes of fresh medium and allowed to progress to G1/S phase. Cells were collected after the release (2 hours for abl cells, 1 hour for C4-2B cells and 1.5 hours for LNCaP cells), stained with propidium iodide (Sigma, St. Louis, MO) and subjected to analysis using a FACS Calibur cell flow cytometer (Becton Dickinson Biosciences, San Diego, CA). FACS analysis was also performed on unsynchronized cells after 13 hours exposure to 50 nM CCI-779.

Cell proliferation assay

Cell proliferation was measured by WST-1 (4-[3-(4-iodophenyl)-2-(4-nitrophenyl)-2H-5-tetrazolio]-1, 3-benzene disulfonate) assay according to the manufacturer's instruction (Roche, Indianapolis, IN). Briefly, this assay entails the addition of 10 μ l WST-1 reagents per 100 μ l cell cultures in a 96-well plate. These cultures were incubated for 30 minutes and the absorbance at 450 nm was determined by an ELISA reader (Bio-Rad, Hercules, CA).

Xenograft model

Male Balb/c athymic nude mice at 6 weeks of age were obtained from Charles River Laboratory (Wilmington, MA) and acclimated for 1 week in a pathogen-free enclosure before start of study. All experiments were conducted in accordance with the guidelines of the Association for Assessment and Accreditation of Laboratory Animal Care International (AAALAC). abl cells (2×10^6 cells / flank) were suspended with 50% Matrigel (Becton Dickinson, Franklin Lakes, NJ) and subcutaneously inoculated bilaterally into the mice flanks, monitored daily and tumor size quantified with calipers twice a week (17, 23). When tumors were grown to 100 mm³, treatments were initiated. Mice were randomly assigned into two cohorts with 10 mice per group. CCI-779 (treated group) or vehicle solution [5%

Tween 80 (Sigma, St. Louis, MO) and 5% polyethylene glycol 400 (Sigma) (13); control group] was given intraperitoneally at the dose of 10 mg/kg for 4 consecutive days per week (24). The injection volume was 0.1ml/10 g. Tumor volume was calculated by using the standard formula: $V = length \times width^2 \times 0.5$. Body weight was also monitored bi-weekly. After 4 weeks, mice were euthanized and tumor tissues were weighed and subjected for western blot analysis.

Transfection and invasion assay

Cells grown in 6-well plates were transfected with siUBE2C or siControl, or 2 μ g of pCS2-myc-UBE2C (kindly provided by Michael Rape, University of California, Berkeley) or a control pCS2-myc vector (a gift from David Turner, University of Michigan) using Lipofectamine 2000 (Invitrogen). Forty-eight hours after transfection, 4×10^5 cells were seeded on the Matrigel-coated filters (BD BioCoat™ BD Matrigel™ Invasion Chamber, Bedford, MA) in the upper chamber, which was filled with media containing 0.1% FBS. The lower chamber was filled with media supplemented with 10% FBS. Both chambers were treated with 50 nM CCI-779 or vehicle. The cells were allowed to invade for 48 hours. The cells on the underside of the filter were then fixed with 80% methanol, stained by 0.3% crystal violet and counted using light microscopy. The invasion results were normalized by cell proliferation under the same treatment conditions.

Chromatin immunoprecipitation (ChIP) and ReChIP

ChIP was performed as previously described (19). The antibodies used were anti-AR (N20), anti-GATA2 (H116), anti-SRC1 (M341), anti-SRC3, anti-p300 (C20), anti-MED1 (M255) from Santa Cruz Biotechnology (Santa Cruz, CA); anti-FoxA1 (ab23738) from Abcam (Cambridge, MA); and anti-RNA pol II (8WG16) from Covance (Berkeley, CA). SRC3 ChIP was performed with SRC3 antibodies as previously described (19). The ChIP-enriched DNA was then quantified by qPCR using specific primers for the UBE2C enhancers 1 and 2 (4), and the UBE2C promoter, respectively. Negative controls used were sequences containing androgen responsive elements (AREs) that do not have actual binding of AR and FoxA1 (4). The primer sequences used in ChIP assay were: UBE2C enhancer 1 (5'-TGCTCTGAGTAGGAACAGGTAAGT-3', and 5'-TGCTTTTTCCATCATGGCAG-3') (4); UBE2C enhancer 2 (5'-CCACAACTCTTCTCAGCTGGG-3', and 5'-TTCTTTCCTTCCCTGTTACCCC-3') (4); UBE2C promoter (5'-GCCCGAGGGAAATTGGAT-3', and 5'-TTACTCCGCGTGGGAACACT-3'); Control ARE region 1 (5'-CACAGAATCAGTCTAGGGTGCTCTT-3', and 5'-CTGCATGCTCAAGGAGTGTGTT-3') (4) and Control ARE region 2 (5'-GCTGATTCAATTACCTCCCAGAA-3', and AGTTTGGGACAGACGGGAAA-3')(4). ReChIP assays were performed as previously described (25).

mRNA stability assay

abl cells were treated with 50 nM CCI-779 or vehicle. At the same time, 5 μ g/ml actinomycin D (Sigma) was used to block mRNA synthesis. Cells were collected at various time points (0, 6, 9, 12, 18 and 24 hours) after treatment and UBE2C mRNA level was quantified by qRT-PCR. The $t_{1/2}$ was calculated using the iterative curve fitting software SigmaPlot (SPSS), by fitting four-parameter exponential decay curves described by formula $y = a * \exp(b / (c * x + d))$. Estimations of c, designated as C, and corresponding standard errors, designated as SE(C), were used to calculate standard error ($t_{1/2} = \log(2) / C$). $t_{1/2} \pm SE(t_{1/2})$ was calculated as $[\log(2) / (C + SE(C)), \log(2) / (C - SE(C))]$.

Results

CCI-779 down-regulates UBE2C protein and mRNA expression levels in CRPC and ADPC cells

Our initial compound screenings for identification of UBE2C inhibitors were performed on abl cells. As a CRPC cell model, abl mimics the clinical properties of a significant proportion of CRPC cases. For example, recent studies reporting that AR upregulates cell-cycle genes (e.g. *UBE2C*, *CDC20* and *CDK1*) in abl cells mimic the pattern of upregulated genes observed in human CRPC versus ADPC cases (4, 7, 8). CCI-779 emerged from screening as it potently decreased both protein and mRNA levels of UBE2C in abl cells (Figs. 1A and 1B). We further extended our study to another CRPC cell model C4-2B that overexpresses the AR (26). We confirmed that UBE2C protein and mRNA levels were significantly decreased in CCI-779 treated C4-2B cells (Figs. 1A and 1B). Interestingly, the inhibitory effect of CCI-779 on UBE2C protein and mRNA levels was also seen in an ADPC cell line LNCaP, although the effect was less effective than that observed in abl and C4-2B cells (Figs. 1A and 1B). Consistent with previous studies showing that mTOR pathway is required for translation of mRNAs of critical G1 phase cell-cycle genes such as *CCND1* (12), we found that treatment of abl, C4-2B and LNCaP cells with CCI-779 significantly reduced CCND1 protein but not mRNA expression level (Figs. 1A and 1B). Thus CCI-779 decreases protein expression levels of both UBE2C and CCND1, and UBE2C mRNA expression level in prostate cancer cells.

To further investigate whether CCI-779-mediated decrease in UBE2C mRNA expression was dependent on CCI-779-induced reduction in CCND1 protein expression, we examined the effect of CCI-779 on UBE2C mRNA level in CCND1 silenced and control silenced abl cells. Silencing of CCND1 caused a complete cell-cycle G1 arrest, which was barely enhanced by CCI-779 treatment (Figs. 1C and 1D). Significantly, treatment of abl cells with CCI-779 decreased UBE2C mRNA level in abl cells already arrested in G1 phase (Fig. 1D). These results indicate that CCI-779 can directly decrease UBE2C mRNA expression in a CCND1 expression- and G1 arrest-independent manner. We obtained essentially similar results in C4-2B cells (Supplementary Fig. S1).

CCI-779 blocks both G2/M and G1/S cell-cycle progression and decreases cell proliferation in CRPC and ADPC cells

As UBE2C plays an essential role in promoting G2/M phase cell-cycle progression in prostate cancer cells (4) and CCI-779 inhibited UBE2C expression (Fig.1), we next examined the effect of CCI-779 on G2/M phase cell-cycle progression. abl, C4-2B and LNCaP cells were synchronized to G2/M phase by using a thymidine-nocodazole block and then released for 1~2 hours. As shown in Fig. 2A, while treatment of cells with CCI-779 had no effect on G2/M synchronization, CCI-779 treatment led to an increase in the G2/M phase and a decrease in the G1 phase after releasing from G2/M synchronization, suggesting that CCI-779 markedly delayed G2/M to G1 transition in all three cell lines. Consistent with the functional role of CCI-779 in decreasing CCND1 protein expression level (Fig. 1A) and a recent study demonstrating that CCI-779 arrests prostate and breast cancer cells in G1/S phase (24), CCI-779 blocked unsynchronized abl, C4-2B and LNCaP cells in G1/S phase (Fig. 2B). The inhibition of CCI-779 on cell-cycle G2/M and G1/S progression was correlated with a significantly decreased cell proliferation of abl, C4-2B and LNCaP (but more notably abl and C4-2B cells) (Fig.2C).

To further delineate the role of UBE2C in CCI-779-mediated CRPC cell proliferation inhibition, the effects of CCI-779 on cell proliferation of UBE2C silenced or control silenced abl and C4-2B cells were examined. The inhibitory effect of CCI-779 on abl cell

proliferation was markedly decreased in UBE2C silenced (28%) versus control silenced (45%) abl cells (Fig. 2D), suggesting that UBE2C silencing-mediated abl cell growth inhibition (Fig. 2D) significantly contributes to growth inhibitory effect of CCI-779 on abl (Fig. 2C). By contrast, as UBE2C silencing only slightly decreased C4-2B cell proliferation (Fig. 2D), CCI-779-mediated inhibition of C4-2B cell proliferation (Fig. 2C) was presumably mostly due to CCI-779-induced decreased expression of CCND1 rather than UBE2C in C4-2B cells (Figs. 1A and 2D).

CCI-779 inhibits *in vivo* growth of abl xenograft through downregulation of UBE2C and CCND1

We further extended our studies to an *in vivo* xenograft model to validate the significance of our *in vitro* findings. Approximately two weeks after the inoculation of abl cells, mice were treated with CCI-779 (10 mg/kg, i.p.) for 4 consecutive days weekly for 4 weeks. Mice generally tolerated CCI-779 without showing any apparent toxicity throughout the experiment. No significant difference in body weight was observed between groups after the four weeks period (data not shown). Remarkably, the tumor growth was inhibited by CCI-779 even after one week of treatment. By the end of the study, the tumor volume dramatically decreased from $234 \pm 33\text{mm}^3$ in control group to $57 \pm 4\text{mm}^3$ in CCI-779-treated group (Figs. 3A and 3B). In addition, there was no measurable tumor in 4 out of 10 CCI-779-treated mice. Tumor weight measurement further supported our findings, as the average value was $78.6 \pm 15.5\text{mg}$ for control group as compared with $13.5 \pm 2.5\text{mg}$ for CCI-779 group (Fig. 3C). More importantly, western blot analysis confirmed that both UBE2C and CCND1 protein levels were significantly decreased in tumor tissues following treatment with CCI-779 (Fig. 3D). These data suggest that CCI-779 significantly decreases CRPC cell *in vivo* growth through inhibition of UBE2C and CCND1. Similar effect of CCI-779 on CRPC cell growth and protein expression of CCND1 and UBE2C was observed in castrated mice (Supplementary Fig. S2).

CCI-779 inhibits UBE2C-dependent CRPC cell invasion *in vitro*

The role of UBE2C is not limited to promoting cell growth. Recent studies have found that UBE2C expression is positively correlated with metastasis in patients with various cancer types, including colorectal cancer (14), breast cancer (15) and soft tissue tumors (16). Consistent with these clinical observations, an *in vitro* study has demonstrated that UBE2C downregulation and overexpression decreases and increases invasiveness of a human colon cancer cell line HT-29, respectively (14). To investigate whether UBE2C expression affects abl, C4-2B and LNCaP cell invasion, we transfected a siRNA targeting UBE2C (siUBE2C) or a control siRNA (siControl), or UBE2C vector or a control vector in all three cell lines (Fig. 4A) followed by Matrigel invasion assays. Control vector or siControl transfected abl and C4-2B cells were significantly more invasive than similarly transfected LNCaP cells (Figs. 4B and 4C, and Supplementary Fig. S3). Interestingly, silencing of UBE2C significantly decreased, whereas overexpression of UBE2C significantly increased invasiveness of abl and C4-2B but not LNCaP cells (Figs. 4B and 4C, and Supplementary Fig. S3), suggesting that UBE2C is necessary for CRPC cell invasion but not sufficient for ADPC cell invasion. It is possible that additional invasion-related proteins are required for UBE2C to mediate ADPC cell invasion. We next examined the effect of CCI-779 on cell invasion. Exposure of control vector transfected abl, C4-2B and LNCaP cells to CCI-779 significantly reduced invasion of abl and C4-2B but not LNCaP cells (Fig. 4C, and Supplementary Fig. S3). Importantly, UBE2C overexpression reversed most of this CCI-779-induced invasion inhibitory effect (Fig. 4C and Supplementary Fig. S3). These results suggest that CCI-779-induced prevention of CRPC cell invasion is mediated mostly by UBE2C.

Mechanisms for CCI-779 inhibition on UBE2C mRNA expression in CRPC cells

To investigate the underlying mechanisms for UBE2C mRNA inhibition by CCI-779 in CRPC cells, we first examined the effect of CCI-779 on recruitment of AR, its collaborating transcription factors FoxA1 and GATA2 (25), and its coactivators histone acetyltransferases (HAT) (SRC1, SRC3, p300), and Mediator subunit (MED1)(19) to the two UBE2C enhancers located -32.8 kb and +41.6 kb away from the transcription start site (TSS) of UBE2C gene in abl cells (4). abl cells were treated with CCI-779, and ChIP assays were performed using antibodies against AR, FoxA1, GATA2, SRC1, SRC3, p300, MED1 and RNA polymerase II (pol II). While exposure to CCI-779 did not affect AR binding at the two UBE2C enhancers, CCI-779 treatment decreased and increased FoxA1/GATA2 recruitment to the UBE2C enhancers 1 and 2, respectively (Figs. 5A-5C). Significantly, CCI-779 treatment attenuated the recruitment of AR coactivators SRC1, SRC3, p300 and MED1 to both UBE2C enhancers but not the two negative control regions (Figs. 5D-5G). Consistent with the notion that HAT modifies chromatin structure to allow Mediator facilitating pol II recruitment to target gene promoters (27-29), exposure to CCI-779 significantly reduced the pol II level at the UBE2C promoter (Fig. 5H).

Since exposure to CCI-779 had no effect on protein expression levels of these coactivators (Fig. 5I), ReChIP assays were performed to investigate whether CCI-779 treatment affected AR-coactivator interaction on chromatin. First-round ChIP was performed with AR or MED1 antibodies, followed by second-round ChIP with p300 or AR antibodies. CCI-779 treatment significantly decreased interactions between AR and p300, and between AR and MED1 (Figs. 5J and 5K), indicating that CCI-779 treatment reduces coactivator binding through disruption of AR-coactivator interactions. Taken together, these data suggest that CCI-779 decreases AR transcription complex loading on UBE2C regulatory regions, which may account, at least in part, for the decreased UBE2C mRNA expression after CCI-779 treatment.

We further addressed whether CCI-779 affects UBE2C mRNA stability in CRPC cells. abl cells were incubated in the presence of either actinomycin D (to block *de novo* transcription)/CCI-779 or actinomycin D/vehicle for 6-24 hours. As shown in Figure 6, the UBE2C mRNA was destabilized by CCI-779 with a $t_{1/2} = 8.52 \pm 0.19$ hours, as compared to the vehicle $t_{1/2} = 10.97 \pm 0.21$ hours. These data suggest that both attenuated gene transcription and mRNA stability contribute to CCI-779 inhibition of UBE2C mRNA level in CRPC cells.

Discussion

The AR is often expressed and functional in most CRPC patients and current clinical studies on CRPC focus on targeting AR itself using AR antagonists [e.g. MDV-3100 (30)] or inhibitors of androgen synthesis [e.g. abiraterone acetate (31)]. Although these agents decrease CRPC growth in some patients, elimination of all AR activity blocks some beneficial actions of AR (e.g. inhibition of some oncogenes like *PCDH11* (32)) and contributes to undesirable effects such as bone loss (33) and metabolic syndrome (34). An alternative approach for the inhibition of cancer promoting AR signaling pathway in CRPC is to target AR downstream target genes involved in CRPC growth. Given our recent findings showing that knocking down of CRPC-specific AR target G2/M phase genes (e.g. *UBE2C*, *CDK1* and *CDC20*) significantly decreases CRPC cell growth (4), we propose that G2/M phase genes could serve as new targets for therapeutic intervention.

In this study, we identified the mTOR inhibitor CCI-779 as an inhibitor for UBE2C in CRPC cells. We showed that CCI-779 treatment significantly decreases UBE2C mRNA and protein expression in CRPC cells at its pharmacologically attainable concentrations in

clinical trials (35, 36) (Fig.1). Although it is well known that inhibition of mTOR decreases protein expression levels of some genes by dephosphorylation of p70 ribosomal S6 kinase (S6K1) and the eukaryotic initiation factor 4E binding protein 1 (4E-BP1)(12, 37), recent studies have found that mTOR inhibitors also decreases RNA levels of some genes (37, 38) through a variety of mechanisms. It has been demonstrated that rapamycin inhibits mitochondrial gene transcription by disruption of protein-protein interactions between a transcription coactivator PGC-1 α and a transcription factor yin-yang 1(YY1), resulting in decreased recruitment of PGC-1 α to the promoters of mitochondrial genes (39). Rapamycin also prevents sterol regulatory element binding protein 1(SREBP1) target gene expression through inhibition of nuclear accumulation of SREBP1 (40). Additionally, rapamycin blocks peroxisome proliferator-activated receptor- γ (PPAR- γ) protein expression leading to decreased PPAR- γ target gene expression (41). With regard to the mechanisms for CCI-779 inhibition of UBE2C mRNA level, while CCI-779 does not affect AR binding and protein expression levels of AR and its coactivators, CCI-779 inhibits the recruitment of AR coactivators to the UBE2C enhancers through disruption of AR-coactivator interactions, leading to decreased pol II loading on the UBE2C promoter (Fig.5). Interestingly, we also found that CCI-779 attenuates UBE2C mRNA stability (Fig.6), suggesting that CCI-779-induced direct downregulation of UBE2C mRNA levels is caused by decreased UBE2C mRNA transcription and stability.

Although mTOR inhibitors have shown great potential as antitumor agents and CCI-779 has been approved by the US Food and Drug Administration (FDA) as the first-line treatment in patients with advanced refractory renal cell cancer (RCC) (11), results from clinical studies on mTOR inhibitors in CRPC have been somewhat disappointing. For example, it was reported that that therapeutic response was observed in only 17%~25% CRPC patients treated with rapamycin alone (42, 43). One of the explanations for such clinical observations is that rapamycin and CCI-779 may activate AR target genes such as *PSA* and *KLK4* in cultured CRPC cells and xenografts, leading to a decreased effect of mTOR inhibitors on inhibition of cell proliferation (42, 44). However, as the AR target genes examined in these studies (42, 44) are not directly relevant to cell growth and invasion, it is not very clear that the failure of mTOR inhibitors as monotherapy is caused by mTOR inhibitor-activated AR signaling. Interestingly, our studies found that CCI-779 significantly decreases the expression of a CRPC-specific AR target gene *UBE2C* in CRPC cell models *abl* and *C4-2B* (Fig. 1). The overexpressed *UBE2C* in *abl* and *C4-2B* cells compared to LNCaP cells (4) plays a critical role in cell proliferation and/or invasion (Figs. 2-4) (4). CCI-779, acting partially through a *UBE2C*-dependent mechanism, significantly decreases *abl* cell growth *in vitro* and *in vivo* (Figs. 2 and 3). Importantly, we also found that CCI-779-induced inhibition of *abl* and *C4-2B* cell invasion is mediated mostly by *UBE2C* (Fig.4). Although the average level of *UBE2C* expression in CRPC patients is significantly higher than that in ADPC patients, *UBE2C* expression in CRPC cases is highly variable (4). Thus it is possible that those CRPC patients with high *UBE2C* expression will have better therapeutic response for CCI-779 than those with low *UBE2C* expression. Future studies will be needed to investigate whether *UBE2C* is able to serve as a biomarker for predicting CCI-779 therapy response in CRPC patients.

Supplementary Material

Refer to Web version on PubMed Central for supplementary material.

Acknowledgments

We thank Dr. Gustavo Leone for helpful discussion, and Hsueh-Li Tan for help with mice castration surgery.

Grant Support

NIH R00 CA126160 (Q.W.), and The Ohio State University Comprehensive Cancer Center (Q.W. and K.K. Chan).

References

1. Heinlein CA, Chang C. Androgen receptor in prostate cancer. *Endocr Rev.* 2004; 25:276–308. [PubMed: 15082523]
2. Knudsen KE, Penning TM. Partners in crime: deregulation of AR activity and androgen synthesis in prostate cancer. *Trends Endocrinol Metab.* 2010; 21:315–24. [PubMed: 20138542]
3. Balk SP, Knudsen KE. AR, the cell cycle, and prostate cancer. *Nucl Recept Signal.* 2008; 6:e001. [PubMed: 18301781]
4. Wang Q, Li W, Zhang Y, et al. Androgen receptor regulates a distinct transcription program in androgen-independent prostate cancer. *Cell.* 2009; 138:245–56. [PubMed: 19632176]
5. Sharma A, Yeow WS, Ertel A, et al. The retinoblastoma tumor suppressor controls androgen signaling and human prostate cancer progression. *J Clin Invest.* 2010; 120:4478–92. [PubMed: 21099110]
6. Ye Y, Rape M. Building ubiquitin chains: E2 enzymes at work. *Nat Rev Mol Cell Biol.* 2009; 10:755–64. [PubMed: 19851334]
7. Varambally S, Yu J, Laxman B, et al. Integrative genomic and proteomic analysis of prostate cancer reveals signatures of metastatic progression. *Cancer Cell.* 2005; 8:393–406. [PubMed: 16286247]
8. Stanbrough M, Bubley GJ, Ross K, et al. Increased expression of genes converting adrenal androgens to testosterone in androgen-independent prostate cancer. *Cancer Res.* 2006; 66:2815–25. [PubMed: 16510604]
9. Reddy SK, Rape M, Margansky WA, Kirschner MW. Ubiquitination by the anaphase-promoting complex drives spindle checkpoint inactivation. *Nature.* 2007; 446:921–5. [PubMed: 17443186]
10. van Ree JH, Jeganathan KB, Malureanu L, van Deursen JM. Overexpression of the E2 ubiquitin-conjugating enzyme UbcH10 causes chromosome missegregation and tumor formation. *J Cell Biol.* 2010; 188:83–100. [PubMed: 20065091]
11. Konings IR, Verweij J, Wiemer EA, Sleijfer S. The applicability of mTOR inhibition in solid tumors. *Curr Cancer Drug Targets.* 2009; 9:439–50. [PubMed: 19442061]
12. Bjornsti MA, Houghton PJ. The TOR pathway: a target for cancer therapy. *Nat Rev Cancer.* 2004; 4:335–48. [PubMed: 15122205]
13. Wu L, Birle DC, Tannock IF. Effects of the mammalian target of rapamycin inhibitor CCI-779 used alone or with chemotherapy on human prostate cancer cells and xenografts. *Cancer Res.* 2005; 65:2825–31. [PubMed: 15805283]
14. Chen S, Chen Y, Hu C, Jing H, Cao Y, Liu X. Association of clinicopathological features with UbcH10 expression in colorectal cancer. *J Cancer Res Clin Oncol.* 2010; 136:419–26. [PubMed: 19779934]
15. Loussouarn D, Campion L, Leclair F, et al. Validation of UBE2C protein as a prognostic marker in node-positive breast cancer. *Br J Cancer.* 2009; 101:166–73. [PubMed: 19513072]
16. Cunha IW, Carvalho KC, Martins WK, et al. Identification of genes associated with local aggressiveness and metastatic behavior in soft tissue tumors. *Transl Oncol.* 2010; 3:23–32. [PubMed: 20165692]
17. Culig Z, Hoffmann J, Erdel M, et al. Switch from antagonist to agonist of the androgen receptor bicalutamide is associated with prostate tumour progression in a new model system. *Br J Cancer.* 1999; 81:242–51. [PubMed: 10496349]
18. Guan YJ, Wang X, Wang HY, et al. Increased stem cell proliferation in the spinal cord of adult amyotrophic lateral sclerosis transgenic mice. *J Neurochem.* 2007; 102:1125–38. [PubMed: 17472707]
19. Wang Q, Carroll JS, Brown M. Spatial and temporal recruitment of androgen receptor and its coactivators involves chromosomal looping and polymerase tracking. *Mol Cell.* 2005; 19:631–42. [PubMed: 16137620]

20. Okamoto Y, Ozaki T, Miyazaki K, Aoyama M, Miyazaki M, Nakagawara A. UbcH10 is the cancer-related E2 ubiquitin-conjugating enzyme. *Cancer Res.* 2003; 63:4167–73. [PubMed: 12874022]
21. Chang TC, Zeitels LR, Hwang HW, et al. Lin-28B transactivation is necessary for Myc-mediated let-7 repression and proliferation. *Proc Natl Acad Sci U S A.* 2009; 106:3384–9. [PubMed: 19211792]
22. Whitfield ML, Zheng LX, Baldwin A, Ohta T, Hurt MM, Marzluff WF. Stem-loop binding protein, the protein that binds the 3' end of histone mRNA, is cell cycle regulated by both translational and posttranslational mechanisms. *Mol Cell Biol.* 2000; 20:4188–98. [PubMed: 10825184]
23. Morton CL, Houghton PJ. Establishment of human tumor xenografts in immunodeficient mice. *Nat Protoc.* 2007; 2:247–50. [PubMed: 17406581]
24. Fung AS, Wu L, Tannock IF. Concurrent and sequential administration of chemotherapy and the Mammalian target of rapamycin inhibitor temsirolimus in human cancer cells and xenografts. *Clin Cancer Res.* 2009; 15:5389–95. [PubMed: 19706800]
25. Wang Q, Li W, Liu XS, et al. A hierarchical network of transcription factors governs androgen receptor-dependent prostate cancer growth. *Mol Cell.* 2007; 27:380–92. [PubMed: 17679089]
26. Sobel RE, Sadar MD. Cell lines used in prostate cancer research: a compendium of old and new lines--part 1. *J Urol.* 2005; 173:342–59. [PubMed: 15643172]
27. Sharma D, Fondell JD. Ordered recruitment of histone acetyltransferases and the TRAP/Mediator complex to thyroid hormone-responsive promoters in vivo. *Proc Natl Acad Sci U S A.* 2002; 99:7934–9. [PubMed: 12034878]
28. Taatjes DJ. The human Mediator complex: a versatile, genome-wide regulator of transcription. *Trends Biochem Sci.* 2010; 35:315–22. [PubMed: 20299225]
29. Malik S, Roeder RG. The metazoan Mediator co-activator complex as an integrative hub for transcriptional regulation. *Nat Rev Genet.* 2010; 11:761–72. [PubMed: 20940737]
30. Tran C, Ouk S, Clegg NJ, et al. Development of a second-generation antiandrogen for treatment of advanced prostate cancer. *Science.* 2009; 324:787–90. [PubMed: 19359544]
31. Attard G, Reid AH, A'Hern R, et al. Selective inhibition of CYP17 with abiraterone acetate is highly active in the treatment of castration-resistant prostate cancer. *J Clin Oncol.* 2009; 27:3742–8. [PubMed: 19470933]
32. Agoulnik IU, Bingman WE 3rd, Nakka M, et al. Target gene-specific regulation of androgen receptor activity by p42/p44 mitogen-activated protein kinase. *Mol Endocrinol.* 2008; 22:2420–32. [PubMed: 18787043]
33. Vanderschueren D, Vandenput L, Boonen S, Lindberg MK, Bouillon R, Ohlsson C. Androgens and bone. *Endocr Rev.* 2004; 25:389–425. [PubMed: 15180950]
34. Braga-Basaria M, Dobs AS, Muller DC, et al. Metabolic syndrome in men with prostate cancer undergoing long-term androgen-deprivation therapy. *J Clin Oncol.* 2006; 24:3979–83. [PubMed: 16921050]
35. Raymond E, Alexandre J, Faivre S, et al. Safety and pharmacokinetics of escalated doses of weekly intravenous infusion of CCI-779, a novel mTOR inhibitor, in patients with cancer. *J Clin Oncol.* 2004; 22:2336–47. [PubMed: 15136596]
36. Hidalgo M, Buckner JC, Erlichman C, et al. A phase I and pharmacokinetic study of temsirolimus (CCI-779) administered intravenously daily for 5 days every 2 weeks to patients with advanced cancer. *Clin Cancer Res.* 2006; 12:5755–63. [PubMed: 17020981]
37. Wullschleger S, Loewith R, Hall MN. TOR signaling in growth and metabolism. *Cell.* 2006; 124:471–84. [PubMed: 16469695]
38. Peng T, Golub TR, Sabatini DM. The immunosuppressant rapamycin mimics a starvation-like signal distinct from amino acid and glucose deprivation. *Mol Cell Biol.* 2002; 22:5575–84. [PubMed: 12101249]
39. Cunningham JT, Rodgers JT, Arlow DH, Vazquez F, Mootha VK, Puigserver P. mTOR controls mitochondrial oxidative function through a YY1-PGC-1alpha transcriptional complex. *Nature.* 2007; 450:736–40. [PubMed: 18046414]

40. Porstmann T, Santos CR, Griffiths B, et al. SREBP activity is regulated by mTORC1 and contributes to Akt-dependent cell growth. *Cell Metab.* 2008; 8:224–36. [PubMed: 18762023]
41. Kim JE, Chen J. regulation of peroxisome proliferator-activated receptor-gamma activity by mammalian target of rapamycin and amino acids in adipogenesis. *Diabetes.* 2004; 53:2748–56. [PubMed: 15504954]
42. Wang Y, Mikhailova M, Bose S, Pan CX, deVere White RW, Ghosh PM. Regulation of androgen receptor transcriptional activity by rapamycin in prostate cancer cell proliferation and survival. *Oncogene.* 2008; 27:7106–17. [PubMed: 18776922]
43. Amato RJ, Jac J, Mohammad T, Saxena S. Pilot study of rapamycin in patients with hormone-refractory prostate cancer. *Clin Genitourin Cancer.* 2008; 6:97–102. [PubMed: 18824432]
44. Kaarbo M, Mikkelsen OL, Malerod L, et al. PI3K-AKT-mTOR pathway is dominant over androgen receptor signaling in prostate cancer cells. *Cell Oncol.* 2010; 32:11–27. [PubMed: 20203370]

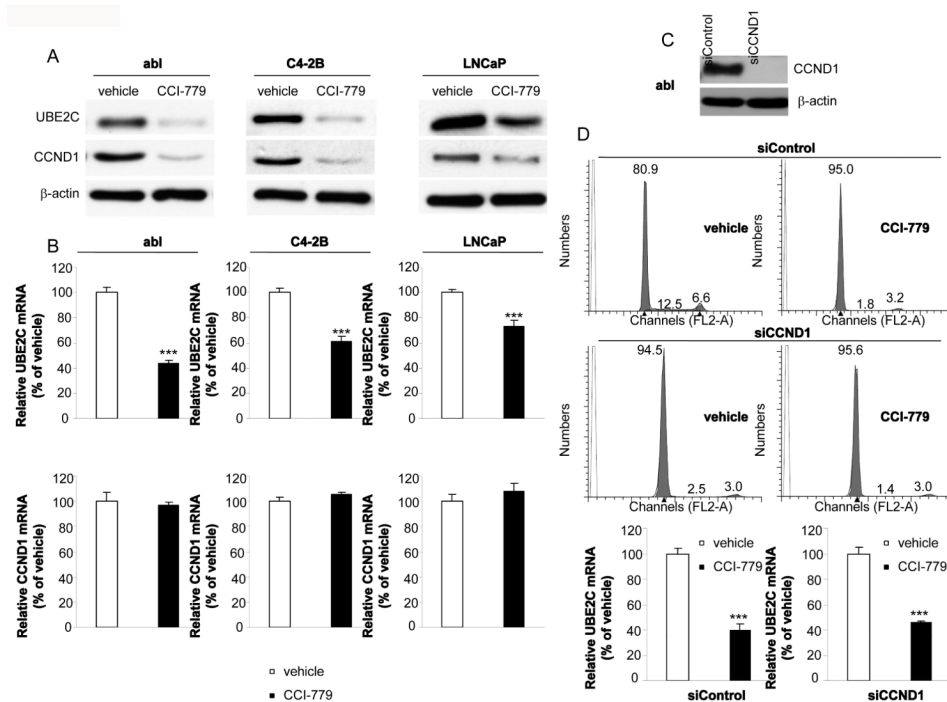
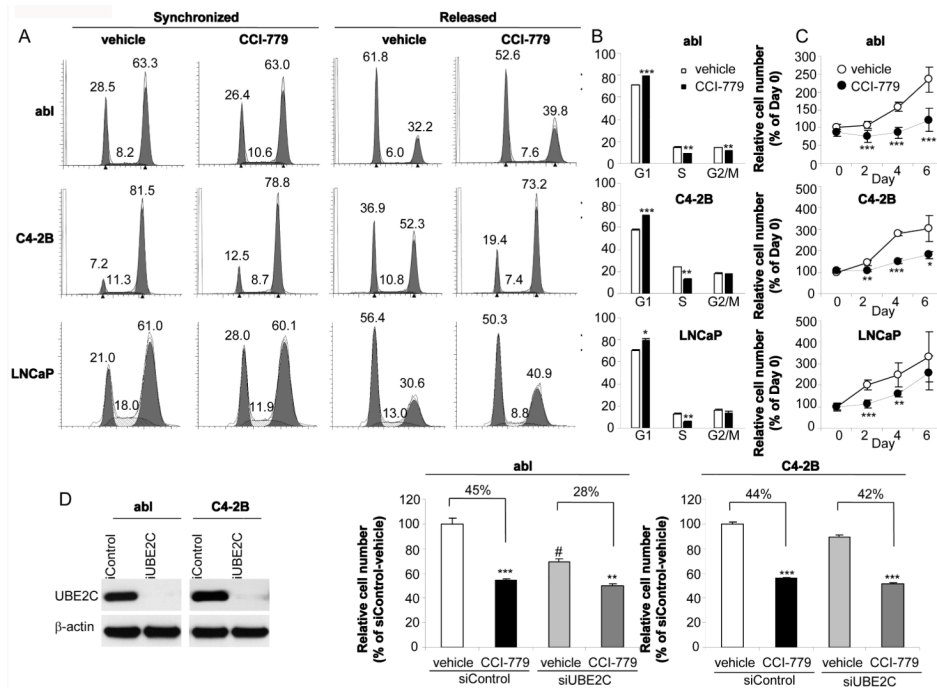


Figure 1.

Effects of CCI-779 on UBE2C and CCND1 expression in CRPC and ADPC cells. A, CCI-779 downregulates protein expression levels of UBE2C and CCND1 in *abl*, C4-2B and LNCaP cell lines. Cells were treated with 50 nM CCI-779 or vehicle for 24 hours and western blot analyses were performed with indicated antibodies. B, CCI-779 decreases mRNA expression level of UBE2C but not CCND1. Cells were incubated with 50 nM CCI-779 for 24 hours. Total RNA was isolated, and analyzed by qRT-PCR using gene-specific primers. The results represent mean \pm SE of three experiments performed in triplicate. *** $p < 0.001$ as compared with the vehicle control. C, Silencing of CCND1 decreases CCND1 protein expression in *abl* cells. *abl* cells were transfected with siControl or siCCND1. Western blots analyses were performed 48 hours after transfection using antibodies indicated. D, CCI-779 decreases UBE2C mRNA expression in both siControl and siCCND1 transfected *abl* cells. Top panel: FACS analyses were performed using siControl or siCCND1 transfected *abl* cells treated with CCI-779 or vehicle for 24 hours. Cell number (%) in each cell cycle phase is indicated in the graph. Lower panel: Total RNA was isolated from siControl or siCCND1 transfected *abl* cells treated with CCI-779 or vehicle for 24 hours. qRT-PCR was then performed using UBE2C-specific primers. *** $p < 0.001$ as compared with the vehicle control.

**Figure 2.**

Effects of CCI-779 on CRPC and ADPC cell-cycle progression and cell proliferation. A, CCI-779 delays cell-cycle G2/M to G1 phase transition. FACS analyses were performed using cells released from thymidine-nocodazole block in the presence or absence of CCI-779 (50 nM). Cell number (%) in each cell cycle phase is indicated in the graph. B, CCI-779 arrests unsynchronized cells in G1/S phase. Thirteen hours after exposure of cells to 50 nM CCI-779, FACS analyses were performed. C, CCI-779 inhibits cell proliferation. Cell proliferation was determined by WST-1 assay on the indicated days (0, 2, 4, 6) in the absence or presence of CCI-779 (50 nM). The data are presented as % of the cell number on Day 0. The results are mean \pm SE of two to three independent experiments performed in triplicate. * $p < 0.05$, ** $p < 0.01$, *** $p < 0.001$ as compared with vehicle control. D, Effects of CCI-779 treatment on cell proliferation of UBE2C silenced and control silenced abl and C4-2B cells. abl or C4-2B cells were transfected with siControl or siUBE2C. Eight-hour posttransfection, cells were treated with CCI-779 or vehicle and cell proliferation assays were performed on Day 4. ** $p < 0.01$, *** $p < 0.001$ as compared with corresponding vehicle control; # $p < 0.001$ as compared with siControl transfected vehicle control.

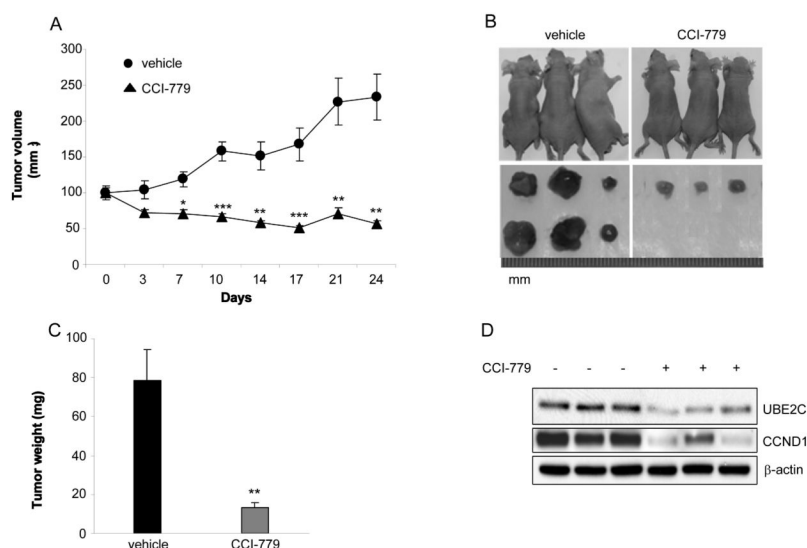


Figure 3.

CCI-779 inhibits *in vivo* CRPC tumor growth through downregulation of UBE2C and CCND1. A, CCI-779 inhibits the growth of subcutaneous *abl* xenograft tumors in nude mice. *abl* cells (2×10^6 /flank) were inoculated into both flanks of male Balb/c nude mice and the treatments were initiated when tumor size reaches 100 mm^3 . The mice were i.p. injected with 10 mg/kg CCI-779 or the vehicle solution for 4 consecutive days every week for 4 weeks (Day 0~3; Day 7~10; Day 14~17; Day 21~24). Tumor volume was measured twice per week and normalized to the percentage of the initial tumor size, which was assigned as 100%. * $p < 0.05$, ** $p < 0.01$, *** $p < 0.001$ compared with vehicle group. $n = 10$ mice for each group. B, Representative images of tumor-bearing mice and their tumors on Day 25 after treatments. C, Average tumor weight for control and CCI-779-treated groups. $n = 16$ for control group; $n = 8$ for CCI-779-treated group. ** $p < 0.01$. D, Western blot analysis shows that CCI-779 reduces protein expression of UBE2C and CCND1 in engrafted tumor tissues. β -actin is a loading control. The blot is representative of two independent experiments.

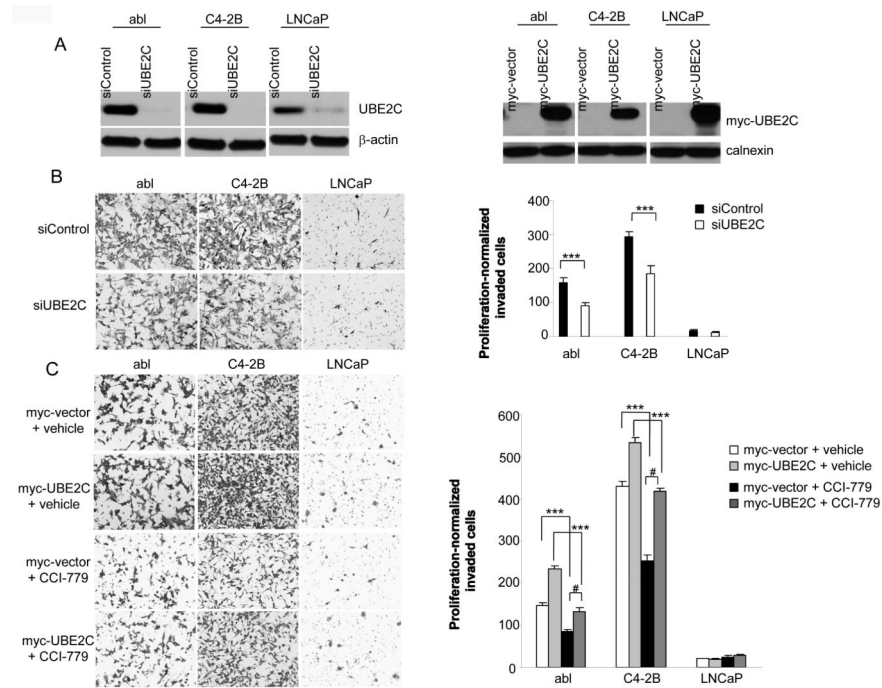
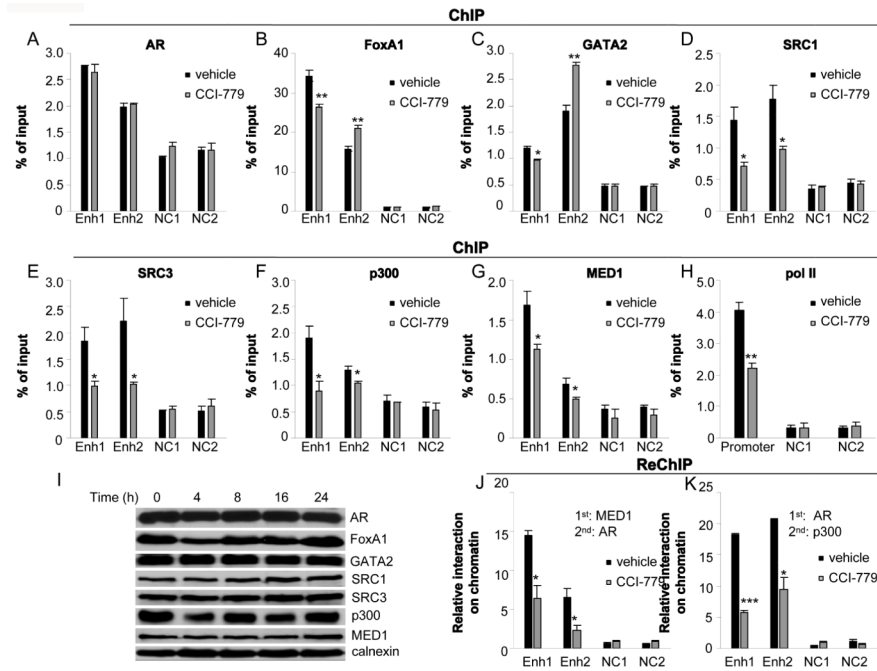


Figure 4.

CCI-779 inhibits UBE2C-dependent CRPC cells invasion *in vitro*. **A**, Left panel: UBE2C silencing decreases UBE2C protein expression. abl, C4-2B and LNCaP cells were transfected with siControl or siUBE2C. Forty-eight hours posttransfection, western blots analyses were performed using antibodies indicated. Right panel: UBE2C overexpression increases UBE2C protein expression. abl, C4-2B and LNCaP cells were transiently transfected with pCS2-myc vector or pCS2-myc-UBE2C. Forty-eight hours later, cell lysates were analyzed by western blot using antibodies indicated. **B**, Left panel: Representative photomicrographs (100 x magnification) show that UBE2C silencing inhibits invasiveness of abl and C4-2B cells. The invaded cells were stained and photographed. Right panel: Quantification of the invaded cells for each cell line after siRNA transfection. The stained cells were manually counted from 5 randomly chosen 100 x fields and normalized with cell proliferation (see Supplementary Fig. S3). *** $p < 0.001$. **C**, Left panel: Representative photomicrographs (100 x magnification) show that CCI-779 inhibits invasion of abl and C4-2B cells and this effect is mostly reversed by UBE2C overexpression. Right panel: Quantification of the invaded cells for each cell line in the absence or presence of CCI-779 (50 nM). The stained cells were manually counted from 5 randomly chosen 100 x fields and normalized with cell proliferation (see Supplementary Fig. S3). *** $p < 0.001$ as compared with vehicle-treated groups; # $p < 0.001$ as compared with CCI-779-treated group without UBE2C overexpression.

**Figure 5.**

CCI-779 inhibits the recruitment of AR coactivators and pol II to UBE2C regulatory regions in CRPC cells. *abl* cells were treated with 50 nM CCI-779 or vehicle for 16 hours and subjected to ChIP analysis with antibodies against AR (A), FoxA1 (B), GATA2 (C), SRC1 (D), SRC3 (E), p300 (F), MED1 (G) or pol II (H), respectively. The DNA precipitates were then quantified by qPCR using primers for the UBE2C enhancers 1 and 2 (Enh 1 and Enh 2), and the UBE2C promoter (mean [n=3] ± SE). Negative controls (NC1 and NC2) are sequences containing AREs, but without actual binding of AR and FoxA1. * $p < 0.05$, ** $p < 0.01$ as compared with vehicle. I, Protein levels of AR, FoxA1, GATA2, SRC1, SRC3, p300 and MED1 remain unchanged following treatment of 50 nM CCI-779 for the indicated time (0, 4, 8, 16, 24 hours). J and K, ReChIP assays were performed with antibodies against MED1 (J) and AR (K) (for first ChIP), and AR (J) and p300 (K) (for ReChIP) (mean [n=3] ± SE). * $p < 0.05$, *** $p < 0.001$ as compared with vehicle.

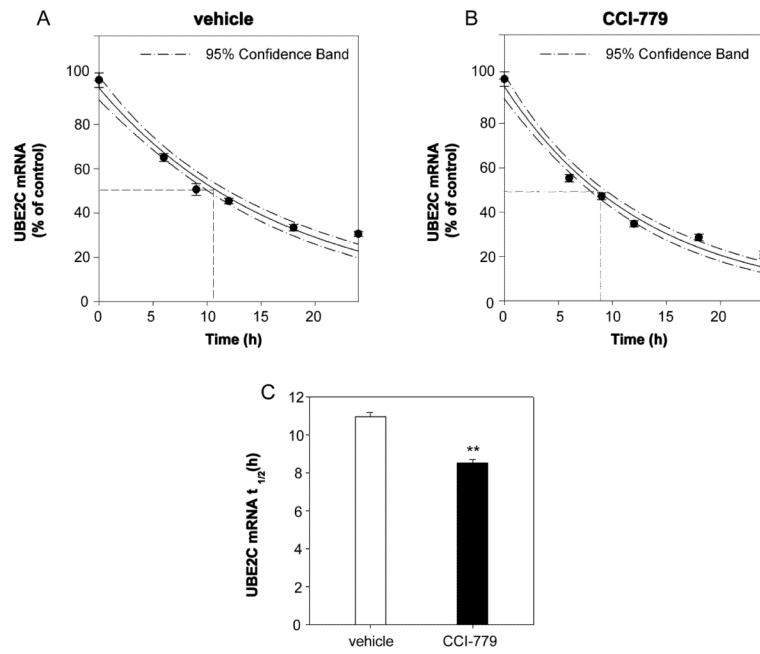


Figure 6. CCI-779 decreases mRNA stability of UBE2C in CRPC cells. A and B, Degradation of UBE2C mRNA in abl cells in the absence or presence of CCI-779. C, CCI-779 shortens the half-life ($t_{1/2}$) of UBE2C mRNA. abl cells were treated with 50 nM CCI-779 or vehicle with transcription blocked by actinomycin D. UBE2C mRNA level was quantified at the indicated time points after actinomycin D treatment. The data are presented as the percentage of the mRNA level measured at time 0 (without adding actinomycin D). ** $p < 0.01$ as compared with vehicle.